ACS OMEGA

Article

Cite This: ACS Omega 2018, 3, 4695−4705

2-Hydroxy-*N*′-((Thiophene-2-yl)methylene)benzohydrazide: Ultrasound-Assisted Synthesis and Corrosion Inhibition Study

Ashish Kumar Singh,*[,†] Sanjeeve Thakur,[‡] Balaram Pani,[§] Eno E. Ebenso,[∥] Mumtaz Ahmad Quraishi,[⊥] and Ajit Kumar Pandey[‡]

[†]Department of Applied Science, Bharati Vidyapeeth's College of Engineering, New Delhi 110063, India

[‡]Department of Chemistry, NSIT, University of Delhi, New Delhi 110078, India

[§]Department of Chemistry, Bhaskaracharya College of Applied Science, University of Delhi, New Delhi 110075, India

[∥]Material Science Innovation & Modelling (MaSIM) Research Focus Area, Faculty of Natural and Agricultural Sciences, North-West University, Private Bag X2046, Mmabatho 2735, South Africa

[⊥]Department of Chemistry, Indian Institute of Technology (BHU), Varanasi 221005, India

Supporting Information

ABSTRACT: 2-Hydroxy-*N*′-((thiophene-2-yl)methylene)-benzohydrazide (HTMBH) was synthesized by conventional method as well as by ultrasonication (US). The ultrasound-assisted synthesis of HTMBH was found to have good yield and be more eco-friendly compared to the conventional method of synthesis. The synthesized compound HTMBH was characterized by Fourier transform infrared, ^{1}H NMR, and CHN analyses. The corrosion inhibition behavior of HTMBH was investigated using gravimetric and electrochemical methods in 0.5 M H_2SO_4. The thermodynamic adsorption parameters revealed that HTMBH was adsorbed on the mild steel surface in both ways, physically and chemically, although physisorption is predominant. The study of activation parameters revealed that it is the increase in activation energy that is a prominent factor to lower the corrosion rate in acid medium. Atomic force microscopy analysis is also carried out to investigate the effect of HTMBH on the surface of mild steel surface in acid solution. The contact angle measurement showed decreased affinity of mild steel surface for acid solution containing HTMBH. The results obtained from all of these methods showed good consistency.

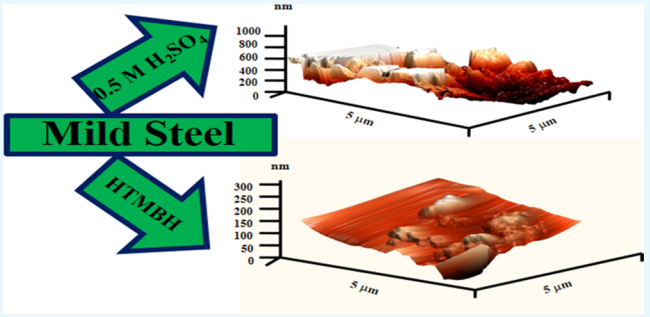

1. INTRODUCTION

The conventional (Con.) methods, which are generally used for a chemical reaction to take place, have some limitations such as energy inefficiency, time consumption, and less yield of product. These shortcomings of the conventional method of synthesis led chemists to look for alternative methods of synthesis, such as exposure to microwave irradiation and ultrasound waves. Sound waves having minimum frequencies to which human ears can respond are considered as ultrasound.[1] The ultrasound wave-assisted method of chemical synthesis is found superior to conventional method as it saves energy and time and results in high yield of desired products. In 1927, Loomis[2] studied and reported the effect of ultrasound waves on chemical reaction. Initially, ultrasound waves were not frequently used, but with progressive development in the field of chemistry, its use has been increased by many folds and lead to a subdiscipline known as sonochemistry.

Ultrasonication (US) has become an important tool in the field of organic synthesis,[3−8] which leads to maximum conversion of reactants into products. Liete et al.[9] reported the ultrasound-mediated synthesis of a variety of aryl hydrazones and found that ultrasound waves considerably reduced the reaction time with improved yield. Thus, ultrasound-mediated synthesis can be considered as a powerful tool for energy conservation and waste minimization.[10−14]

The importance of Schiff bases has been increased by many folds in recent years.[15] The importance and application of Schiff bases has ever attracted enormous research interest and created huge scope for future research. Schiff bases have shown a number of industrial applications as well as biological activities, such as antimicrobial, antibacterial, antifungal, antitumor, anticancer,[16] and antimalarial.[17−19] Schiff bases having thiophene nucleus have been very important for study because these compounds can be used as a structural unit to synthesize charge-transporting molecules, which can be used in transistors, light-emitting diodes, and organic solar cells.[20−23] Thiophene nucleus has very promising characteristic[24] and therefore can be considered as a significant topic of study in the field of

Received: January 1, 2018
Accepted: March 15, 2018
Published: April 30, 2018

DOI: 10.1021/acsomega.8b00003
ACS Omega 2018, 3, 4695−4705

heterocyclic chemistry. The lone pairs of electrons present on an S atom are more effectively delocalized in the heterocyclic ring compared to other heteroatoms such as O and N in case of furan and pyrrole because of the larger size of S atom. A variety of Schiff bases with thiophene moiety have been synthesized, which are very versatile especially for producing a variety of biologically active complexes.[25−28]

The chemical properties of hydrazones have been intensively studied in several research fields because of their high physiological activity and chelating capability.[29] Acid hydrazide and hydrazones have shown a number of applications in biological as well as analytical chemistry.[30−36] A variety of Schiff bases have been studied as corrosion inhibitors recently.[37−40] The inhibition property of Schiff bases is due to the presence of C═N bond.[41,42]

Corrosion has always been a major problem of metallic structure because economic cost due to corrosion failure is so high; furthermore, it leads to public risk, so it is time to develop some novel substances that can retard corrosion of metallic structure especially in acidic medium. Organic compounds especially those having heteroatom, such as N, O, S, and P, have been frequently used as corrosion inhibitor to mitigate corrosion because of their effectiveness, ease of use, and economic aspect. Further, the presence of heteroatoms acts as an active center to be adsorbed on the metallic surface and mitigate the metallic corrosion.[43,44]

Thus, in view of the importance of hydrazide and hydrazones, we have synthesized benzohydrazide with thiophene moiety and investigated its anticorrosion behavior against corrosion of mild steel in 0.5 M H_2SO_4. We have chosen this molecule to examine its anticorrosion performance because of the presence of aromatic ring, nitrogen atoms, and thiophene nucleus, which makes adsorption easier on the surface of mild steel. In addition to these features, the presence of a vacant 3d orbital of S atom of thiophene creates the possibility of formation of $d_\pi-d_\pi$ bond with 3d electrons of Fe. In view of importance of green chemistry and cleaner environment, we have synthesized 2-hydroxy-*N*′-((thiophene-2-yl)methylene)benzohydrazide (HTMBH) by an ultrasound-assisted method using ethanol as a solvent and evaluated its corrosion inhibition effect against mild steel corrosion in acid medium.

2. RESULTS AND DISCUSSION

2.1. Synthesis. The studied inhibitor 2-hydroxy-*N*′-((thiophen-2-yl)methylene)benzohydrazide (HTMBH) was synthesized according to the reaction scheme presented in Figure 1. The starting material thiophene-2-carboaxaldehyde (A) was allowed to react with 2-hydroxybenzoylhydrazide (B) by the following two methods. In the first method, thiophene-2-carboaxaldehyde (A) was refluxed with 2-hydroxybenzohydrazide (B) in a round-bottom flask using glacial acetic acid as a catalyst for 3 h, resulting in the production of HTMBH, whereas the same product HTMBH can also be produced by the second method, which involved ultrasound irradiation of A with B in ethanol for 4 min. The second method considerably reduced the reaction time (from 3 h to 4 min) as well as greatly enhanced the yield of product. The use of ultrasound waves appreciably increases the yield of the product (from 78% in conventional method to 95% in ultrasound-assisted method) and decreases the reaction time (from 3 h to 4 min). So, it provides a faster and cleaner methodology for the synthesis of the studied compound HTMBH compared to the conventional method.

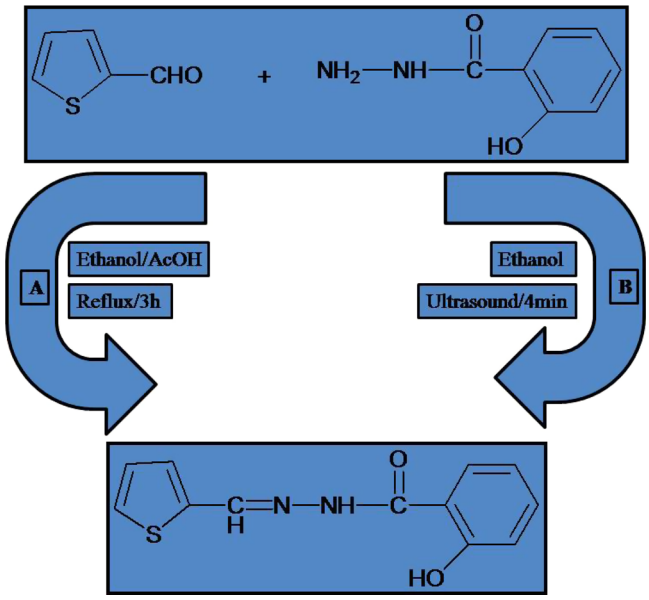

Figure 1. Route of synthesis of compound HTMBH by (A) conventional method and (B) ultrasound-assisted method.

The Fourier transform infrared spectra of the compound HTMBH shows absorption bands at 3450, 3250, 1654, 1630, and 998 cm^{-1} (as presented in Table 1), which are assigned to ν(OH), ν(NH), ν(C═O), ν(C═N), and ν(N−N), respectively. The absence of NH_2 peak, which was originally present in *ortho*-hydroxybenzohydrazide, indicates that it is condensed with the carbonyl group of thiophene nucleus. The presence of a peak at 1630 cm^{-1} is assigned to C═N, which clearly indicates the formation of Schiff base HTMBH.

The ^{1}H NMR spectrum of HTMBH shows resonance signals between 7.86 and 7.68 ppm, which are assigned to phenyl ring protons. A low-field signal at 10.90 ppm reveals the presence of secondary amino proton (−NH), which confirms the presence of keto form of HTMBH; if enolization would have taken place, then −NH proton would have been disappeared. A signal appears at 12.30 ppm, which confirmed the presence of −OH proton. The signal appearing between 6.92 and 6.97 ppm confirms the presence of thiophene ring protons.

2.2. Electrochemical Study. *2.2.1. Electrochemical Impedance Spectroscopy (EIS).* The open corrosion potential (OC_RP) is considered as a parameter that decides the tendency of a material to be oxidized in any corrosive medium.[45,46] This potential is a function of time as the surface of material changed with time. The working electrode was immersed in acid solution in the absence and presence of different concentrations of HTMBH before running each and every electrochemical experiment and its open-circuit potential (OCP) was recorded after 180 min. After this elapsed time interval, a stable and constant open corrosion potential related to corrosion potential (E_{corr}) was attained. Electrochemical impedance spectroscopy (EIS) has been used as a significant tool in corrosion and solid-state laboratories.[47] Electrochemical impedance spectroscopy was performed to throw some light into the correlation between electrochemical measurements and corrosion rates. The EIS experiments were carried out for mild steel samples immersed in 0.5 M H_2SO_4 having different concentrations of HTMBH. The EIS images for MS with varying concentration

DOI: 10.1021/acsomega.8b00003
ACS Omega 2018, 3, 4695−4705

Table 1. Yield and Physical Data of the Product HTMBH

	time		yield%					
product	Con. (h)	US (min)	Con.	US	M.P. (°C)	IR[a] (ν cm^{-1}, KBr)	^{1}H NMR[a] (DMSO-d_6; δ ppm)	CHN[a] (%)
HTMBH	2	4	78	95	246	ν(OH) 3450b;	10.90 (s, 1H, NH)	C = 58.78
						ν(NH) 3250b;	12.30 (s, 1H, OH)	H = 4.11
						ν(C═O) 1654s;	8.66 (1H, CH═N)	N = 11.58
						ν(C═N) 1630s;	7.86–7.68 (4H, aromatic protons)	S = 13.01
						ν(N–N) 998w	6.92–6.97 (3H, thiophene protons)	

[a]IR of HTMBH obtained from ultrasound assisted method.

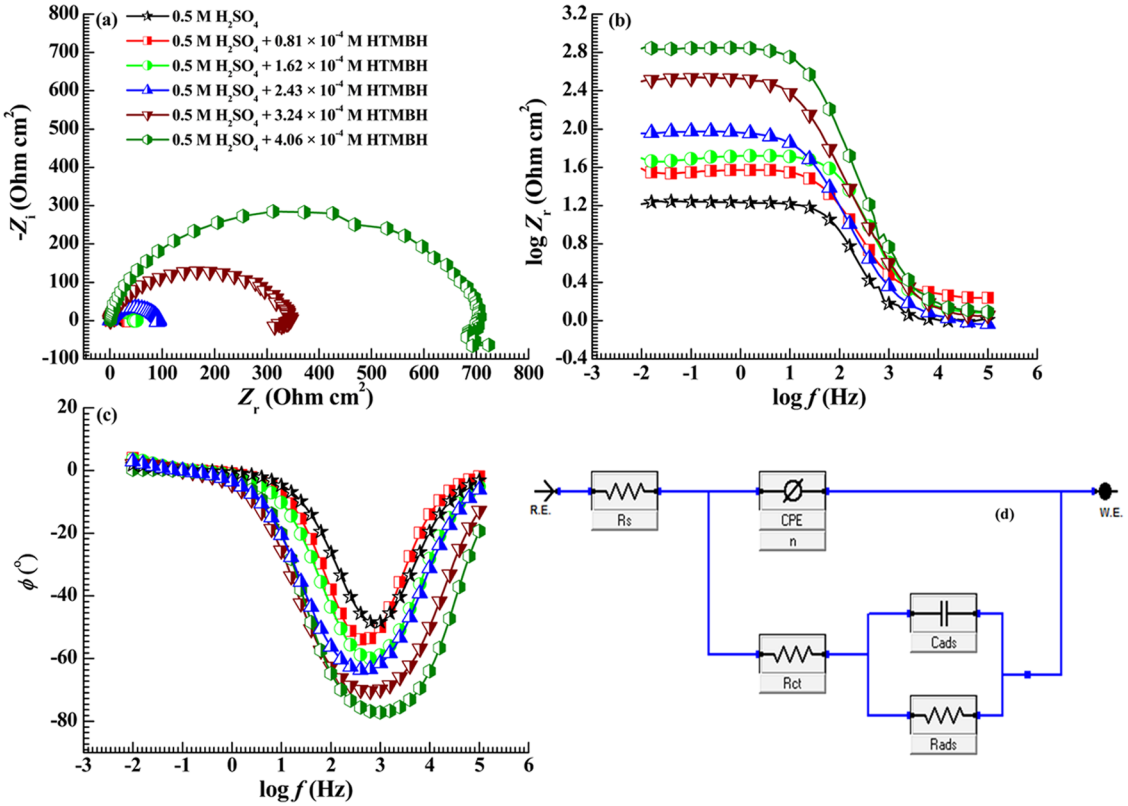

Figure 2. (a) Nyquist plots, (b) Bode magnitude plot, (c) phase angle plot for the corrosion of mild steel in 0.5 M H_2SO_4 in the absence and presence of different concentrations of HTMBH, and (d) equivalent circuit proposed to fit the EIS experimental data.

Table 2. Impedance Parameters for Mild Steel in 0.5 M H_2SO_4 in the Absence and Presence of Different Concentrations of Studied Inhibitor HTMBH

conc. of HTMBH (M × 10^{-4})	R_s (Ω cm^2)	R_{ct} (Ω cm^2)	n	Y_0 (10^{-6} Ω^{-1} cm^{-2})	C_{dl} (μF cm^{-2})	C_{ads} (F cm^{-2})	R_{ads} (Ω cm^2)	R_p (Ω cm^2)	η_{EIS}%
	0.97	16.29	0.824	225.5	68.1	−11.70	−3.39	12.91	
0.81	1.69	36.27	0.825	179.2	62.6	−0.29	−3.22	33.05	60.93
1.62	1.13	51.60	0.843	142.9	57.2	−0.13	−5.39	46.21	72.06
2.43	0.89	92.02	0.859	103.2	48.0	−2.33	−9.62	82.39	84.33
3.24	1.00	339.80	0.872	69.6	40.2	−0.38	−27.64	312.16	95.86
4.06	1.12	694.9	0.907	13.0	8.0	−0.58	−10.60	684.30	98.11

of HTMBH are presented in Figure 2a–c. An equivalent circuit, which is used to analyze the impedance data, is presented in Figure 2d. Different impedance parameters calculated by fitting the data to a given equivalent circuit and corrosion inhibition efficiency using EIS data are presented in Table 2. The impedance data can be used to calculate the corrosion inhibition efficiency of inhibitor as

$$\eta_{EIS}\% = \frac{R_p^i - R_p^0}{R_p^i} \times 100 \quad (1)$$

where R_p^i and R_p^0 are polarization resistances in the presence and absence of inhibitor, respectively. The sum of adsorption resistance (R_{ads}) and charge-transfer resistance (R_{ct}) gives the value of polarization resistance, R_p. The increasing value of R_p with increasing concentration of HTMBH indicates that it is the charge-transfer process that controls the corrosion of mild steel.

DOI: 10.1021/acsomega.8b00003
ACS Omega 2018, 3, 4695−4705

As seen in Figure 2, the Nyquist plot consists of a high-frequency capacitive loop and a low-frequency inductive loop. Increasing concentration of HTMBH resulted in increased diameter of capacitive loop, which is an indication of increased effectiveness of HTMBH against corrosion of mild steel. The low-frequency inductive loop is obtained due to either adsorption of M^{2+} (Fe^{2+}) or relaxation of already adsorbed species, such as SO_4^{2-} and H^+_{ads}.[48]

The increment of impedance or decrease in C_{dl} (double-layer capacitance) with increasing HTMBH concentration, as observed in Table 2, is due to adsorption of the same on MS surface, resulting in increased thickness of the double layer. The relation between double-layer capacitance, C_{dl}, and thickness of the protective layer is given by eq 2.[49]

$$\delta_{org} = \frac{\varepsilon_0 \varepsilon_r}{C_{dl}} \tag{2}$$

where δ_{org} is the thickness of the protective layer, ε_0 is the dielectric constant, and ε_r is the relative dielectric constant.

Theoretically, an ideal Nyquist plot should be a semicircle having its center on x axis. Observation of the Nyquist plots obtained revealed that they are depressed semicircle with its center below x axis. This is due to either heterogeneity of electrode surface or distribution of resistivity or other physical property of the system. Thus, constant phase element (CPE) is used to replace ideal capacitance in equivalent circuit.[50]

A CPE's impedance can be calculated using eq 3

$$\frac{1}{Z} = Y = Q^0(j\omega)^n \tag{3}$$

where Q^0 is equal to reciprocal of impedance ($1/|Z|$) for ω = 1 rad s^{-1}.

The decreasing value of Y with increasing inhibitor concentration (presented in Table 2) indicates more adsorption of inhibitor HTMBH molecule on the surface of mild steel.

The value of n decides the behavior of CPE;[51] for n = 0, 1, −1, and 0.5, the CPE represents resistance, capacitance, inductance, and Warburg impedance, respectively. The value of n ranged from 0.825 to 0.907, which confirmed the capacitive behavior of this system. Examination of Table 2 reveals that the value of n is increased by increasing the concentration of HTMBH, which is an indication of increasing capacitive behavior of this system. The C_{dl} values can be calculated using CPE parameters as

$$C_{dl} = (Y_0 R_{ct}^{1-n})^{1/n} \tag{4}$$

The phase angle decreased by the addition of inhibitor HTMBH (Figure 2c), which is attributed to increase in capacitive behavior at the metal solution interface due to decreased MS dissolution rate.

2.2.2. Potentiodynamic Polarization. The potentiodynamic polarization curves for mild steel in 0.5 M H_2SO_4 with different concentrations of HTMBH are presented in Figure 3. The polarization parameters, i.e., corrosion potential (E_{corr}), corrosion current density (i_{corr}), and cathodic and anodic Tafel slopes (β_c and β_a, respectively), are given in Table 3. The inhibition efficiency using corrosion current density can be calculated using eq 5

$$\eta_{PDP}\% = \frac{i^0_{corr} - i^i_{corr}}{i^0_{corr}} \times 100 \tag{5}$$

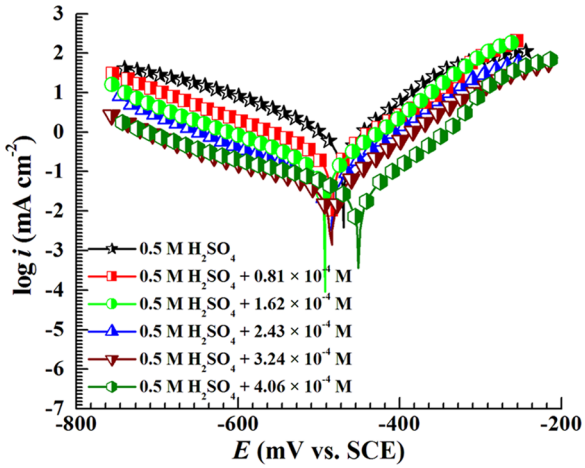

Figure 3. Tafel polarization curves for mild steel in 0.5 M H_2SO_4 acid solution in the absence and presence of different concentrations of HTMBH.

In the presence of inhibitor HTMBH, the corrosion current, cathodic or anodic, decreases (given in Table 3), resulting in reduced corrosion rate. Also, examination of Tafel slope indicated that anodic slope is relatively constant except at 1.62×10^{-4} M HTMBH concentration. The relatively constant values of anodic Tafel slope indicate that it simply blocked the reaction sites of MS surface and thereby lowered the corrosion rate. The increased value of cathodic Tafel slope, β_c, with inhibitor HTMBH compared to that in 0.5 M H_2SO_4 indicates that the mechanism of cathodic reaction is affected, i.e., higher energy will be required for evolution of H_2 gas. The relatively higher value of anodic Tafel slope at 1.62×10^{-4} M HTMBH concentration might be due to change of chemical to electrochemical mechanism. The values of corrosion potential (E_{corr}) are not changed significantly; the change in E_{corr} ranged from 3 to 47 mV, which is less than 85 mV,[52,53] confirming the mixed-type nature of the studied inhibitor HTMBH. The results obtained from gravimetric analysis, electrochemical impedance spectroscopy (EIS), and Tafel polarization showed good consistency.

2.3. Gravimetric Analysis. To evaluate relationship between anticorrosion performance of HTMBH and its concentration, gravimetric analyses have been performed with different amounts of HTMBH in 0.5 M H_2SO_4. It was found that the studied compound has increasing efficiency with increasing concentration (Figure 4a). The result of weight loss study presented in Figure 4b clearly indicates that the rate of corrosion mitigated considerably with an increasing amount of studied compound HTMBH. This result supports the view that at higher concentration the HTMBH molecule adsorbed more effectively on the MS surface and results in reduced corrosion rate, which takes place initially due to adsorption of the anion of the acid used, i.e., SO_4^{2-}. Different experimental results showed good consistency (Figure 5).

2.3.1. Adsorption Isotherm. Corrosion inhibition is mainly due to adsorption and therefore it is usually studied through adsorption isotherm,[54] i.e., relation between amounts of adsorbate adsorbed on the surface of adsorbent. Depending on the forces acting between adsorbate and adsorbent, adsorption is of two types: physical adsorption or physisorption and chemical adsorption or chemisorption. Physisorption involves simple van der Waals forces or electrostatic interaction

DOI: 10.1021/acsomega.8b00003
ACS Omega 2018, 3, 4695−4705

Table 3. Tafel Polarization Parameters for Mild Steel in the Absence and Presence of Different Concentrations of HTMBH in 0.5 M H_2SO_4

conc. of HTMBH (M × 10^{-4})	$-E_{corr}$ (mV vs SCE)	i_{corr} (μA cm^{-2})	β_a (mV dec^{-1})	β_c (mV dec^{-1})	η_{PDP}%
	469	731	73.0	127.0	
0.81	484	313	90.0	141.0	57.2
1.62	514	224	133.0	155.0	69.3
2.43	492	132	71.0	137.0	81.9
3.24	445	43	67.3	172.3	94.1
4.06	422	34	70.0	178.0	95.3

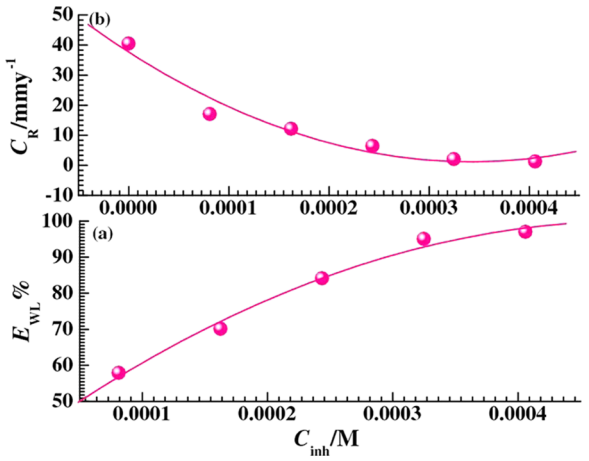

Figure 4. Variation of (a) inhibition efficiency and (b) corrosion rate of HTMBH in 0.5 M H_2SO_4 acid solutions in the absence and presence of different concentrations of HTMBH.

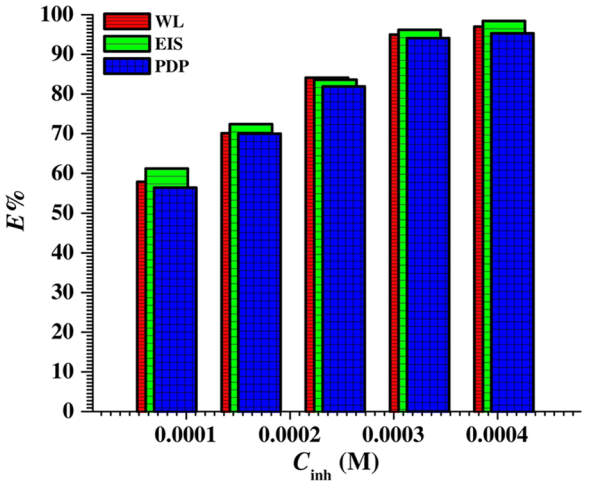

Figure 5. Efficiency of HTMBH in 0.5 M H_2SO_4 acid solution obtained by different methods.

between adsorbate and adsorbent, whereas chemisorption involves chemical forces between them.[55] In this study, several adsorption isotherms were tested to fit the experimental data, but Langmuir adsorption isotherm provides the best linear fit as its linear correlation coefficient is close to unity.

The general form of the Langmuir equation is shown below

$$\frac{C_{inh}}{\theta} = \frac{1}{K_{ads}} + C_{inh} \quad (6)$$

where θ is the number of sites on the mild steel (adsorbent) on which inhibitor molecules are adsorbed, C_{inh} is the inhibitor concentration present in bulk of the solution, and K_{ads} is the equilibrium constant for distribution of inhibitor HTMBH molecule between mild steel surface and bulk of the acid solution. The Langmuir adsorption isotherm plot for adsorption of HTMBH is shown in Figure 6a. The intercept of Langmuir isotherm gives the value of K_{ads} (presented in Table 4), which is related to Gibb's free energy of adsorption by eq 7[56]

$$\Delta G^\circ_{ads} = -RT \ln(55.5K_{ads}) \quad (7)$$

where 55.5 is the amount of water in bulk of solution.

This value of free energy (ΔG°_{ads}) gives the idea about interaction between adsorbate and adsorbent, i.e., HTMBH and the mild steel surface. In general, −20 kJ mol^{-1} or less indicates physical interaction between adsorbate and adsorbent, whereas −40 kJ mol^{-1} or more indicates chemical interaction between them. The value of ΔG°_{ads} (given in Table 4) in our study indicates that HTMBH interacted with mild steel surface in both ways, i.e., physisorption and chemisorption are involved during interaction of HTMBH to MS surface. The high value of K_{ads} and ΔG°_{ads} indicated strong interaction of HTMBH molecule with MS surface and hence its high inhibition efficiency is justified.

It is well known that corrosion inhibition of metal and alloy using inhibitors is due to adsorption of inhibitors on the metal surface. Actually, it is solvent, i.e., water molecule, which could also be adsorbed on metal surface; thus, adsorption of inhibitor can be considered as a competitive phenomenon, which depends on the composition of molecule, electrochemical potential, and physical environment, i.e., temperature of the solution.

The adsorption of molecule to the metal surface can be regarded as

$$Org_{aq} + xH_2O_{ads} \leftrightarrow xH_2O_{aq} + Org_{ads} \quad (8)$$

where x is the number of water molecules displaced by one molecule of inhibitor present in the bulk of the solution to be adsorbed.

The anticorrosion performance of HTMBH can be better explained by considering thermodynamic parameters. The equilibrium constant for adsorption−desorption process, K_{ads}, is related to enthalpy of adsorption according to eq 9

$$\ln K_{ads} = \frac{-\Delta H^\circ_{ads}}{RT} + \text{constant} \quad (9)$$

The plot of ln K_{ads} versus $1/T$ is presented in Figure 6b with a slope value equal to $-\Delta H^\circ_{ads}/R$. The value of ΔH°_{ads} is given in Table 4. The low value of ΔH°_{ads} confirms that HTMBH is adsorbed on the mild steel surface largely by physisorption.

To calculate activation parameters of corrosion, gravimetric analyses were performed at different temperatures, i.e., 303−333 K. The activation parameters can be calculated from corrosion rate as[57]

DOI: 10.1021/acsomega.8b00003
ACS Omega 2018, 3, 4695−4705

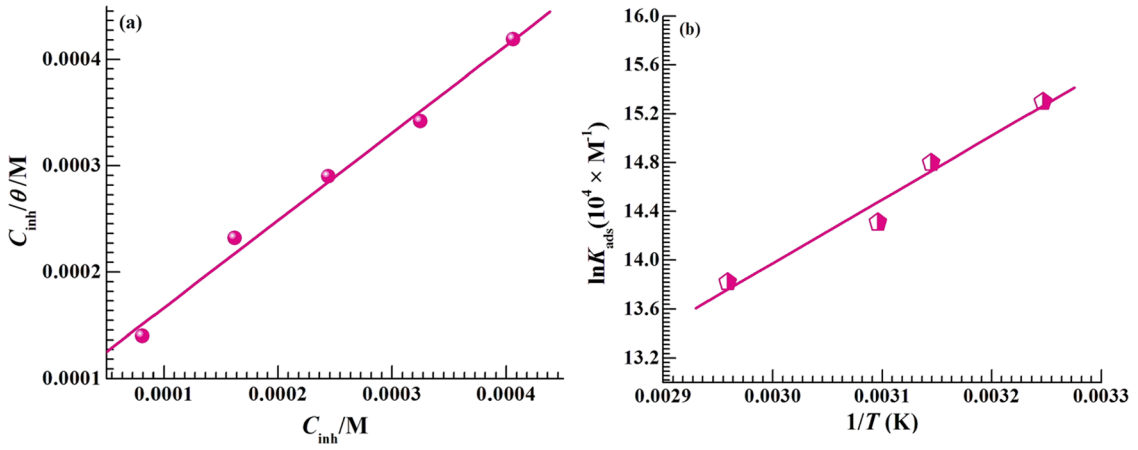

Figure 6. (a) Langmuir adsorption isotherm plots for the adsorption of HTMBH on the surface of mild steel and (b) adsorption isotherm plot for ln K_{ads} vs $1/T$.

Table 4. Thermodynamic Adsorption Parameters for Adsorption of HTMBH on Mild Steel in 0.5 M H_2SO_4

conc. of HTMBH (M × 10^{-4})	temperature (K)	K_{ads} (10^4 × M^{-1})	$-\Delta G^{\circ}_{ads}$ (kJ mol^{-1})	ΔH°_{ads} (kJ mol^{-1})
4.06	303	7.95	39.18	−26.06
	313	4.82	39.12	
	323	2.95	39.01	
333	1.80	38.85		

$$\log(C_R) = \frac{-E_a}{2.303RT} + \log \lambda \quad (10)$$

$$C_R = \frac{RT}{Nh} \exp\left(\frac{\Delta S^*}{R}\right) \exp\left(-\frac{\Delta H^*}{RT}\right) \quad (11)$$

where R is the gas constant, T is the absolute temperature, C_R is the corrosion rate, and λ is the pre-exponential factor. The plots of log C_R versus $1/T$ and log C_R/T versus $1/T$ for mild steel in 0.5 M H_2SO_4 having different concentrations of HTMBH are presented in Figure 7. The values of activation parameters calculated from these two plots are presented in Table 5. The increased value of activation energy in the presence of inhibitor HTMBH compared to bare acid solution indicates that energy barrier for occurrence of corrosion is increased.

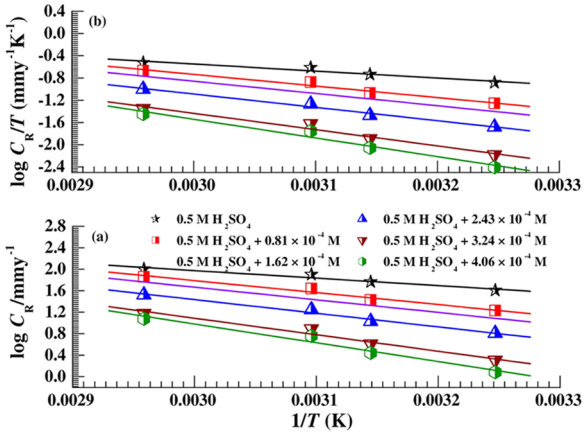

Figure 7. Arrhenius plots (a) log C_R vs $1/T$ and (b) log C_R/T vs $1/T$ for carbon steel in 0.5 M H_2SO_4 in the absence and presence of different concentrations of HTMBH.

Table 5. Activation Parameters for Mild Steel Corrosion in 0.5 M H_2SO_4 in the Absence and Presence of HTMBH

conc. of HTMBH (M × 10^{-4})	E_a (kJ mol^{-1})	λ (mg cm^{-2})	ΔH^* (kJ mol^{-1})	$-\Delta S^*$ (J mol^{-1} K^{-1})
	26.72	4.74 × 10^2	23.99	−136.05
0.81	42.70	4.81 × 10^3	39.97	−91.69
1.62	44.93	6.04 × 10^3	42.20	−87.34
2.43	48.60	8.52 × 10^3	45.86	−80.76
3.24	58.86	3.00 × 10^4	56.13	−56.60
4.06	67.06	9.78 × 10^4	64.33	−34.03

The increase in the value of ΔH^*, presented in Table 5, in the presence of HTMBH, confirmed its high protection efficiency. The negative value of ΔS^* as given in Table 5 proves that randomness of activated complex is reduced compared to that of reactant; further increased values of ΔS^* at higher concentration of the studied inhibitor HTMBH indicates that the presence of higher concentration of HTMBH led to competitive adsorption equilibrium between inhibitor molecule present in bulk of the solution and water molecules already adsorbed on the surface of mild steel. The entropy of activation is actually the algebraic sum of entropy of inhibitor and solvent; thus, increase in entropy is only due to increased entropy of solvent molecule.

2.4. Morphological Study. *2.4.1. Atomic Force Microscopy (AFM).* In recent years, atomic force microscopy (AFM) has been used frequently to investigate the surface morphology. The AFM images of MS surface are presented in Figure 8. The average surface roughness of MS sample before immersion in acid solution was 58 nm (Figure 8a). The average surface roughness of mild steel coupon immersed in acid solution with HTMBH (Figure 8b) is 338 nm, which can be considered as smooth surface compared to the one immersed in acid solution with average surface roughness of 570 nm (Figure 8c).

2.4.2. Scanning Electron Microscopy (SEM). Scanning electron micrographs were scanned to study the effect of HTMBH on the surface morphology of mild steel. The scanning electron micrography image of mild steel surface immersed in bare acid solution is shown in Figure 9a, whereas that of mild steel surface immersed in 0.5 M H_2SO_4 with 4.06 × 10^{-4} M HTMBH is shown in Figure 9b. Examination of Figure 9 revealed that the surface of mild steel coupon immersed in acid solution with inhibitor HTMBH is comparatively less damaged (Figure 9b) compared to the one immersed in bare

DOI: 10.1021/acsomega.8b00003
ACS Omega 2018, 3, 4695−4705

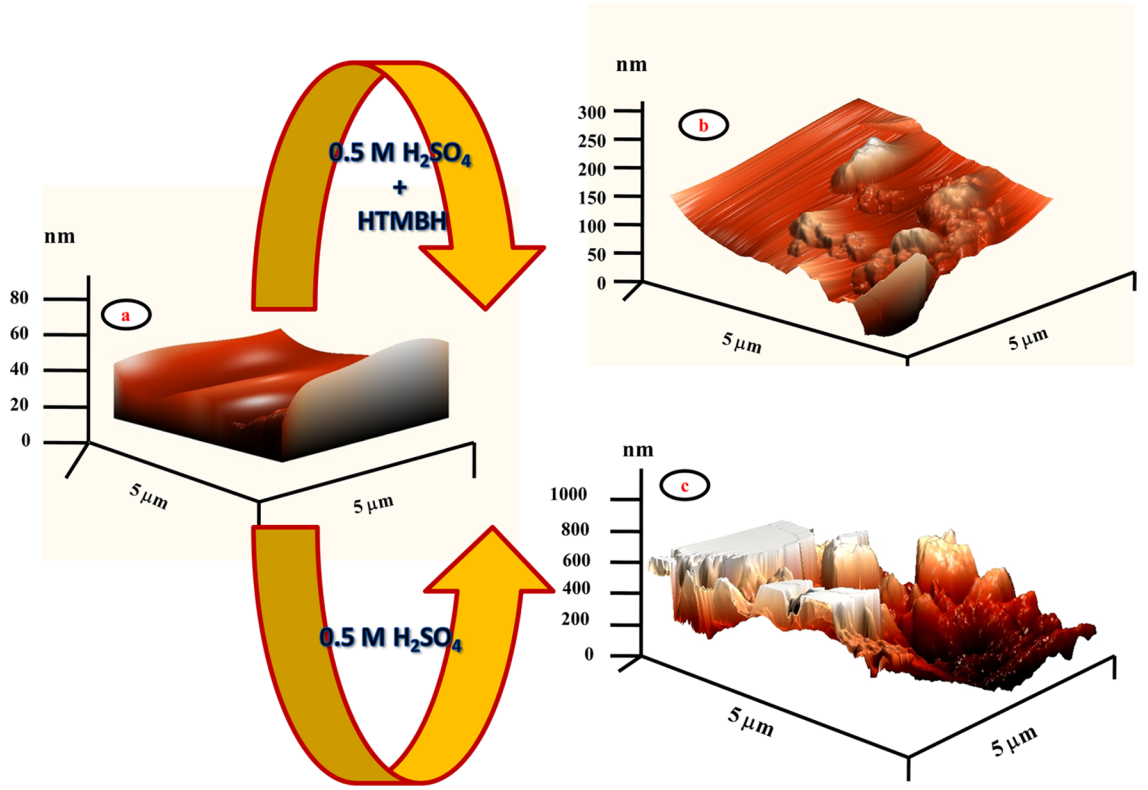

Figure 8. Atomic force micrography images of (a) mild steel before immersion in 0.5 M H_2SO_4, (b) after immersion in inhibited solution, and (c) after immersion in bare acid solution.

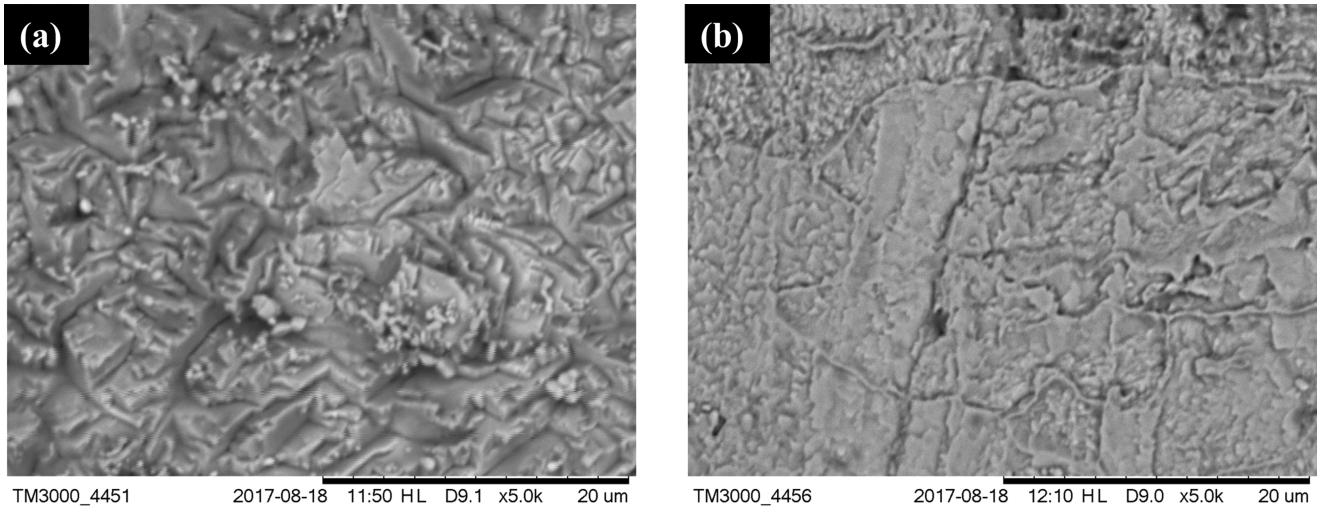

Figure 9. SEM images of mild steel sample after immersion in (a) 0.5 H_2SO_4 and (b) 0.5 M H_2SO_4 + 4.06 × 10^{-4} M HTMBH.

acid solution (Figure 9a), which confirms the inhibitive action of HTMBH.

2.5. Contact Angle Measurement. The results of contact angle measurement are presented in Figure 10. The least contact angle for bare acid solution confirms the maximum affinity of mild steel surface to the bare acid solution having no inhibitor. The contact angle decreased gradually by addition of inhibitor HTMBH, which means that mild steel surface showed lower affinity to the acid solutions having inhibitor HTMBH.

3. CORROSION INHIBITION MECHANISM

The mechanism of corrosion inhibition of mild steel by 2-hydroxy-*N*′-((thiophene-2-yl)methylene)benzohydrazide (HTMBH) in acid solution was established by corrosion reaction kinetics obtained from electrochemical measurements.

In general, corrosion inhibitor mitigates corrosion in one of the following ways:

(i) Inhibitor reduces the corrosion rate by adsorption on the metal surface.[58]

(ii) It may lead to the formation of oxide film of the base metal.[59]

DOI: 10.1021/acsomega.8b00003
ACS Omega 2018, 3, 4695−4705

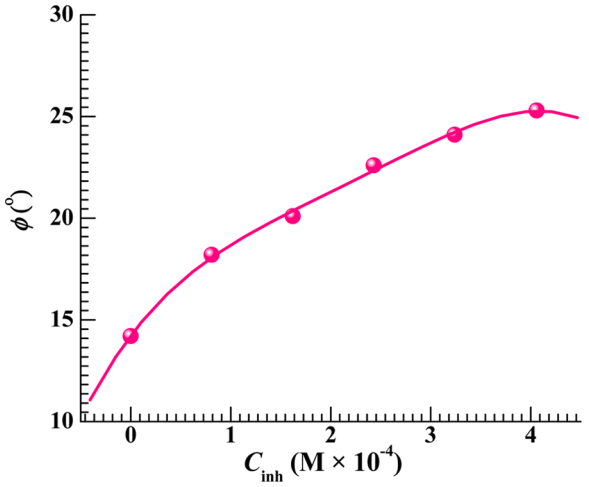

Figure 10. Variation of contact angle of electrolytic solution with different concentrations of HTMBH at the mild steel surface.

(iii) It may also react with corrosive component present in corrosive medium and result into a complex.[60]

The organic corrosion inhibitors adsorbed on the metal surface thereby mitigate the corrosion rate. It is well accepted that adsorption of corrosion inhibitor is a competitive phenomenon replacing water molecules already adsorbed on the metal surface and subsequently adsorbed itself according to eq 8.

The adsorption of inhibitor molecule on the mild steel surface may take place in a number of methods as follows:

(i) May adsorb electrostatically on the metal surface.
(ii) May adsorb by donation of unshared electron pair located on heteroatoms or π-electrons of aromatic system to vacant 3d orbital of iron.
(iii) Retro donation may also be attributed for adsorption of inhibitor molecule on the surface of mild steel.

Examination of the structure of HTMBH reveals that the presence of C═N facilitates physical interaction, whereas unshared electron pairs located on heteroatom and π-electrons led to chemical interaction with the mild steel surface. Similar findings were reported earlier by other researchers.[61,62] The HTMBH was found superior compared to some earlier studied hydrazones of furfuraldehyde[63] and benzaldehyde.[64] The possibility of the $d_\pi - d_\pi$ bonding between 3d electrons of Fe atom and vacant 3d orbitals of S atom of thiophene nucleus is attributed for the appreciable efficiency of HTMBH at higher concentrations even at higher temperature. Such type of inhibitors which not only offer d-electrons but also have vacant d-orbitals to accept metal electrons forming stable chelates, which have already been studied as excellent inhibitors.[65]

4. CONCLUSIONS

1. Ultrasound-assisted synthesis of HTMBH was found more productive compared to conventional method.
2. Although the cathodic reaction of corrosion is more prominently affected, the shift of corrosion potential confirmed the mixed-type nature of HTMBH inhibitor.
3. Langmuir adsorption isotherm is followed by adsorption of HTMBH on the mild steel surface in sulfuric acid medium.
4. The increase in activation energy in the presence of inhibitor HTMBH lowers the corrosion rate.
5. The low value of enthalpy of adsorption (≈26 KJ mol^{-1}) indicates that HTMBH is adsorbed on the mild steel surface largely by physical method.
6. The results of electrochemical and surface study were well supported by the data of contact angle measurements.

5. EXPERIMENTAL PROCEDURE

5.1. Synthesis of 2-Hydroxy-*N*′-((thiophene-2-yl)-methylene)benzohydrazide (HTMBH). In the present study, thiophene-2-carboxaldehyde is allowed to react with *ortho*-hydroxybenzohydrazide conventionally[66] as well as by ultrasound-assisted method in ethanol to get 2-hydroxy-*N*′-((thiophene-2-yl)methylene)benzohydrazide (HTMBH) in reasonably good yield. All of the spectral data (IR, ^{1}H NMR, and CHN analyses) of the synthesized compound were according to its assigned structure. The physical data and yield of the synthesized compound (of both methods: conventional and ultrasound-assisted) are given in Table 1.

In conventional method, thiophene-2-carboxaldehyde is refluxed with *ortho*-hydroxybenzohydrazide in ethanolic solution in the presence of glacial acetic acid as a catalyst in a round-bottom flask. The reaction mixture was cooled after refluxing, and a yellow product was obtained.

The uncorrected melting point of the synthesized compound HTMBH was measured in an open capillary. The spectral data of HTMBH were recorded as earlier[67] using a JASCO FT/IR-5300 spectrophotometer for IR and a Jeol AL 300 FTNMR for ^{1}H NMR spectra. The elemental analysis data were obtained using Exeter Analytical Inc. model CE-440 CHN analyzer. All of the required chemicals to synthesize HTMBH were supplied from Sigma-Aldrich.

5.2. Corrosion Inhibition Study. *5.2.1. Electrochemical Study.* The electrochemical study was performed using a three-electrode cell consisting of saturated calomel electrode as the reference one, mild steel as the working electrode, and a Pt foil of 1 cm^2 size as the counter electrode. All of the electrochemical studies were performed under nonstirring condition after immersing the mild steel (working) electrode in 0.5 M H_2SO_4 for 180 min so that it could attain stable corrosion potential. Gamry potentiostat/galvanostat (model 300) with DC 105 and Echem Analyst software was used to perform all of the electrochemical experiments.

Stock solution of HTMBH was made in 0.5 M H_2SO_4. This solution was used for all electrochemical and gravimetric experiments.

To record electrochemical impedance spectroscopy (EIS) measurements, the frequency was kept in the range of 100 kHz to 0.01 Hz with an alternating current voltage amplitude of 0.01 V at E_{corr} under potentiostatic condition. All of the EIS data were tested for fitting of appropriate equivalent circuit using software Echem Analyst. The potentiodynamic polarization curves were scanned as described elsewhere.[68]

5.2.2. Gravimetric analysis. The aggressive solution of acid (0.5 M) was made from 98% H_2SO_4 supplied from E. Merck. The weight loss experiments were carried out with different concentrations of HTMBH ranged from 0.81×10^{-4} to 4.06×10^{-4} M according to ASTM G-31[69] using stock solution of HTMBH. The mild steel sheet of composition (by weight): C, 0.17; Mn, 0.46; Si, 0.26; S, 0.017; P, 0.019; remaining Fe was used for all of the experiments. The mild steel sheet of above composition was cut into coupons of $2.5 \times 2.0 \times 0.025$ cm^3 size

DOI: 10.1021/acsomega.8b00003
ACS Omega 2018, 3, 4695−4705

and used further for gravimetric analysis. These mild steel coupons were abraded first by emery paper of grade 200−1200 and then used for gravimetric analysis.

The inhibition efficiency of the studied compound HTMBH based on gravimetric method can be calculated using the equation[70]

$$\eta_{WL}\% = \frac{w_0 - w_i}{w_0} \times 100 \quad (12)$$

where w_0 and w_i are the weight loss values in the absence and presence of HTMBH, respectively.

5.3. Morphological Study. *5.3.1. Atomic Force Microscopy (AFM).* To investigate the effect of HTMBH on the surface morphology of mild steel, atomic force micrographs of different mild steel coupons immersed in 0.5 M H_2SO_4 in the absence and presence of the studied inhibitor were scanned. These micrographs were recorded by an NT-MDT multimode atomic force microscope, with frequency in the range of 2.4−2.5 × 10^5 Hz and spring constant of 11.5 N m^{-1}. All of the images were interpreted by NOVA software.[71] The standard tips were used in semicontact mode to scan topographical images. Prior to recording topographical images, mild steel samples were immersed in bare 0.5 M H_2SO_4 acid solution and acid solution having 4.06 × 10^{-4} M HTMBH for 3 h; then, they are taken out, washed, and dried. These dried mild steel samples were used to record topographical images.

5.3.2. Scanning Electron Microscopy (SEM). The scanning electron micrographs were also scanned to study the effect of HTMBH on the surface morphology of mild steel in acidic medium. The mild steel specimens were prepared as for AFM and scanned with a TM 3000 scanning electron microscope with an acceleration voltage of 5000 V and a working distance of 8.5 mm.

5.3.3. Contact Angle Measurement. To evaluate the affinity of mild steel surface for acid solutions with varying concentration of inhibitor, contact angles were measured by a Rame−Hart goniometer (Netcong) by a static sessile drop technique, which is normally used for characterization of solid as well as liquid surface energies. The mild steel samples were cleaned properly with acetone to assure the mild steel surface free of dust, grease, and organic traces, which can influence the contact angle measurement. The cleaned mild steel samples were then used to measure contact angle.

■ ASSOCIATED CONTENT

Supporting Information

The Supporting Information is available free of charge on the ACS Publications website at DOI: 10.1021/acsomega.8b00003.

^{1}H NMR spectra of the studied compound (PDF)

■ AUTHOR INFORMATION

Corresponding Author

*E-mail: ashish.singh.rs.apc@itbhu.ac.in. Tel: +919560285447.

ORCID

Ashish Kumar Singh: 0000-0001-8076-0816

Eno E. Ebenso: 0000-0002-0411-9258

Notes

The authors declare no competing financial interest.

■ ACKNOWLEDGMENTS

A.K.S. acknowledges Bharati Vidyapeeth's College of Engineering for providing platform to carry out this research. The authors are immensely grateful to reviewers for their comments that greatly improved the manuscript. E.E.E. acknowledges the NRF of South Africa for incentive funding for rated researchers.

■ REFERENCES

(1) Singh, V.; Kaur, K. P.; Khurana, A.; Kad, G. L. Ultrasound: a boon in the synthesis of organic compounds. *Resonance* **1998**, *3*, 56−60.

(2) Richards, W. T.; Loomis, A. L. The chemical effects of high frequency sound waves I. A preliminary survey. *J. Am. Chem. Soc.* **1927**, *49*, 3086−3100.

(3) Hobuss, C. B.; Venzke, D.; Pacheco, B. S.; Souza, A. O.; Santos, M. A. Z.; Moura, S.; Quina, F. H.; Fiametti, K. G.; Oliveira, J. V.; Pereira, C. M. P. Ultrasound-assisted synthesis of aliphatic acid esters at room temperature. *Ultrason. Sonochem.* **2012**, *19*, 387−389.

(4) Fan, X.; Chen, F.; Wang, X. Ultrasound-assisted synthesis of biodiesel from crude cottonseed oil using response surface methodology. *J. Oleo Sci.* **2010**, *59*, 235−241.

(5) Vieira, B. M.; Thurow, S.; Costa, M. D.; Casaril, A. M.; Domingues, M.; Schumacher, R. F.; Perin, G.; Alves, D.; Savegnago, L.; Lenardao, E. J. Ultrasound-Assisted Synthesis and Antioxidant Activity of 3-Selanyl-1 H-indole and 3-Selanylimidazo[1,2-a]pyridine Derivatives. *Asian J. Org. Chem.* **2017**, 1635.

(6) Masoomi, M. Y.; Morsali, A.; Junk, P. C. Ultrasound assisted synthesis of a Zn(II) metal−organic framework with nano-plate morphology using non-linear dicarboxylate and linear N-donor ligands. *RSC Adv.* **2014**, *4*, 47894−47898.

(7) Suresh; Sandhu, S. Ultrasound-assisted synthesis of 2, 4-thiazolidinedione and rhodanine derivatives catalyzed by task-specific ionic liquid: [TMG][Lac]. *Org. Med. Chem. Lett.* **2013**, *3*, 2−7.

(8) Vassilev, D.; Petkova, N.; Koleva, M.; Denev, P. Ultrasound-Assisted Synthesis of Sucrose and Fructooligosaccharides Esters as Bio-Plasticizers. *J. Renewable Mater.* **2016**, *4*, 24−30.

(9) Leite, A. C. L.; Moreira, D. R. d. M.; Coelho, L. C. D.; de Menezes, F. D.; Brondani, D. J. Synthesis of aryl-hydrazones via ultrasound irradiation in aqueous medium. *Tetrahedron Lett.* **2008**, *49*, 1538−1541.

(10) De Oliveira, A. S.; Llanes, L. C.; Nunes, R. J.; Yunes, R. A.; Brighente, I. M. C. Use of Ultrasound and Microwave irradiation for Clean and Efficient Synthesis of 3,3′-(Arylmethylene)bis(2-hydroxynaphthalene-1,4-dione)Derivatives. *Green Sustainable Chem.* **2014**, *04*, 177−184.

(11) Arafa, W. A. A.; Shaker, R. M. A facile green chemistry approaches towards the synthesis of bis-Schiff bases using ultrasound versus microwave and conventional method without catalyst. *Arkivoc* **2016**, 187−201.

(12) Banerjee, B. Recent developments on ultrasound assisted catalyst-free organic synthesis. *Ultrason. Sonochem.* **2017**, *35*, 1−14.

(13) Poddar, M. K.; Arjmand, M.; Sundararaj, U.; Moholkar, V. S. Ultrasound-assisted synthesis and characterization of magnetite nanoparticles and poly(methyl methacrylate)/magnetite nanocomposites. *Ultrason. Sonochem.* **2018**, *43*, 38−51.

(14) Crawford, D. E. Solvent-free sonochemistry: Sonochemical organic synthesis in the absence of a liquid medium. *Beilstein J. Org. Chem.* **2017**, *13*, 1850−1856.

(15) Kajal, A.; Bala, S.; Kamboj, S.; Sharma, N.; Saini, V. Schiff Bases: A Versatile Pharmacophore. *J. Catal.* **2013**, *2013*, No. 893512.

(16) Patil, S.; Kuman, M. M.; Palvai, S.; Sengupta, P.; Basu, S. Impairing Powerhouse in Colon Cancer Cells by Hydrazide−Hydrazone-Based Small Molecule. *ACS Omega* **2018**, *3*, 1470−1481.

(17) Pandeya, S. N.; Sriram, D.; Nath, G.; De Clercq, E. Synthesis, antibacterial, antifungal and anti-HIV evaluation of Schiff and Mannich bases of satin derivative with 3-amino-2-methylmercapto quinazolin-4 (3H)−one. *Pharm. Acta Helv.* **1999**, *74*, 11−17.

DOI: 10.1021/acsomega.8b00003
ACS Omega 2018, 3, 4695−4705

(18) Singh, U. K.; Pandeya, S. N.; Singh, A.; Srivastava, B. K.; Pandey, M. Synthesis and Antimicrobial Activity of Schiff's and N-Mannich Bases of Isatin and Its Derivatives with 4-Amino-N-Carbamimidoyl Benzene Sulfonamide. *Int. J. Pharm. Sci. Drug Res.* **2010**, *2*, 151−154.
(19) Sahu, S. K.; Azam, M. A.; Banerjee, M.; Acharrya, S.; Behera, C. C.; Sic, S. Synthesis, Characterization and Biological Activity of 2-Methyl-3-aminoquinazolin-4(3H)-ones Schiff Bases. *J. Braz. Chem. Soc.* **2008**, *19*, 963−970.
(20) Bolduc, A.; Mallet, C.; Skene, W. G. Survey of recent advances of in the field of π-conjugated heterocyclic azomethines as materials with tuneable properties. *Sci. China Chem.* **2013**, *56*, 3−23.
(21) Wong, W. Y.; Wang, X. Z.; He, Z.; Chan, K. K.; Djurisic, A. B.; Cheung, K. Y.; Yip, C. T.; Ching, A. M.; Xi, Y. Y.; Mak, C. S. K.; Chan, W. K. Tuning the Absorption, Charge Transport Properties, and Solar Cell Efficiency with the Number of Thienyl Rings in Platinum-Containing Poly(aryleneethynylene)s. *J. Am. Chem. Soc.* **2007**, *129*, 14372−14380.
(22) Zhang, F.; Sun, B.; Song, T.; Zhu, X.; Lee, S. Efficient Hybrid Photovoltaic Devices Based on Poly (3-hexylthiophene) and Silicon Nanostructures. *Chem. Mater.* **2011**, *23*, 2084−2090.
(23) Ghosh, T.; Panicker, J. S.; Nair, V. C. Self-Assembled Organic Materials for Photovoltaic Application. *Polymers* **2017**, *9*, 112−151.
(24) Mishra, R.; Jha, K. K.; Kumar, S.; Tomer, I. Synthesis, properties and biological activity of thiophene: A review. *Der Pharma Chem.* **2011**, *3*, 38−54.
(25) Sztanke, K.; Maziarka, A.; Osinka, A.; Sztanke, M. An insight into synthetic Schiff bases revealing anti proliferative activities in vitro. *Bioorg. Med. Chem.* **2013**, *21*, 3648−3666.
(26) Bhattacharjee, S.; Saravanan, J.; Mohan, S.; Arrora, M. Synthesis, Charecterization and CNS depressant activity of some Schiff bases of 2-amino-N-(o-Fluoro phenyl acetamido) 4-(p-methoxyphenyl) thiophenes. *Int. J. Pharm. Sci.* **2012**, *4*, 528−532.
(27) Sani, B. P.; Dawson, M. I.; Hobbs, P. D.; Chan, R. L. S.; Schiff, L. J. Relationship between binding affinities to cellular retinoic acid-binding protein and biological potency of a new series of retinoids. *J. Cancer Res.* **1984**, *44*, 190−195.
(28) Raj, K. M.; Vivekananda, B.; Nagesh, G. Y.; Mruthyunjayaswamy, B. H. M. Synthesis, spectroscopic characterization, electrochemistry and biological evaluation of some binuclear transition metal complexes of bicompartmental ONO donor ligands containing benzo[b]thiophene moiety. *J. Mol. Struct.* **2014**, *1059*, 280−293.
(29) Lindoy, L. F.; Livingstone, S. E. Complexes of iron(II), cobalt (II), and nickel (II) with α-di-imines and related bidentate ligands. *Coord. Chem. Rev.* **1967**, *2*, 173−193.
(30) Sah, P. P. T.; Peoples, S. A. Isonicotinylhydrazones as antitubercular agents and derivatives for idendification of aldehydes and ketones. *J. Am. Pharm. Assoc.* **1954**, *43*, 513−524.
(31) Küçükgüzel, S. G.; Mazi, A.; Sahin, F.; Öztürk, S.; Stables, J. Synthesis and biological activities of diflunisal hydrazide-hydrazones. *Eur. J. Med. Chem.* **2003**, *38*, 1005−1013.
(32) Popiołek, Ł. Hydrazide−hydrazones as potential antimicrobial agents: overview of the literature since 2010. *Med. Chem. Res.* **2017**, *26*, 287−301.
(33) Narang, K. K.; Pandey, J. P.; Singh, K. P.; Rai, P. K. Synthesis, Characterization, IR and Electronic Spectra, Magnetic Moments and Biological Activity of Trinuclear Nickel(II) TetrathiocyanatoBisArgentate(I) Complexes with Hydrazides and Hydrazones. *Synth. React. Inorg. Met.−Org. Chem.* **1990**, *20*, 1301−1316.
(34) Katyal, M.; Dutt, Y. Analytical applications of hydrazones. *Talanta* **1975**, *22*, 151−166.
(35) Singh, R. B.; Jain, P.; Singh, R. P. Hydrazones as analytical reagents: a review. *Talanta* **1982**, *29*, 77−84.
(36) Liu, F.; Stephen, A. G.; Adamson, C. S.; Gousset, K.; Aman, M. J.; Freed, E. O.; Fisher, R. J.; BurkeJr, T. R. Hydrazone- and Hydrazide-Containing N-Substituted Glycines as Peptoid Surrogates for Expedited Library Synthesis: Application to the Preparation of Tsg101-Directed HIV-1 Budding Antagonists. *Org. Lett.* **2006**, *8*, 5165−5168.
(37) Erami, R. S.; Amirnasr, M.; Raeissi, K.; Momeni, M. M.; Meghdadi, S. Multidentate Schiff bases as new and effective corrosion inhibitors for mild steel in hydrochloric acid solution: an electrochemical and quantum chemical assessment. *J. Iran Chem. Soc.* **2015**, *12*, 2185−2197.
(38) Menaka, R.; Subhasini, S. Chitosan Schiff base as effective corrosion inhibitor for mild steel in acid medium. *Polym. Int.* **2017**, *66*, 349−358.
(39) Khan, G.; Basirun, W. J.; Kazi, S. N.; Ahmed, P.; Magaji, L.; Ahmed, S. M.; Khan, G. M.; Rehman, M. A.; Badry, A. B. B. M. Electrochemical investigation on the corrosion inhibition of mild steel by Quinazoline Schiff base compounds in hydrochloric acid solution. *J. Colloid Interface Sci.* **2017**, *502*, 134−145.
(40) Saha, S. K.; Dutta, A.; Ghosh, P.; Sukul, D.; Banerjee, P. Novel Schiff-base molecules as efficient corrosion inhibitors for mild steel surface in 1 M HCl medium: experimental and theoretical approach. *Phys. Chem. Chem. Phys.* **2016**, *18*, 17898−17911.
(41) Daoud, D.; Douadi, T.; Issaadi, S.; Chafaa, S. Adsorption and corrosion inhibition of new synthesized thiophene Schiff base on mild steel X52 in HCl and H_2SO_4 solutions. *Corros. Sci.* **2014**, *79*, 50−58.
(42) Fouda, A. S.; Ismail, M. A.; Abousalem, A. S.; Elewadya, G. Y. Experimental and theoretical studies on corrosion inhibition of 4-amidinophenyl-2,20-bifuran and its analogues in acidic media. *RSC Adv.* **2017**, *7*, 46414−46430.
(43) Bedaira, M. A.; El-Sabbaha, M. M. B.; Foudab, A. S.; Elaryian, H. M. Synthesis, electrochemical and quantum chemical studies of some prepared surfactants based on azodye and Schiff base as corrosion inhibitors for steel in acid medium. *Corros. Sci.* **2017**, *128*, 54−72.
(44) Gupta, N. K.; Verma, C.; Quraishi, M. A.; Mukherjee, A. K. Schiff's bases derived from l-lysine and aromatic aldehydes as green corrosion inhibitors for mild steel: Experimental and theoretical studies. *J. Mol. Liq.* **2016**, *215*, 47−57.
(45) Fernandez-Solis, C. D.; Vimalanandan, A.; Altin, A.; Mondragon-Ochoa, J. S.; Keil, K. K.; Erbe, A. Fundamentals of Electrochemistry, Corrosion and Corrosion Protection. In *Soft Matter at Aqueous Interfaces*; Lang, P. R., Liu, Y., Eds.; Springer International Publishing: Switzerland, 2016.
(46) Matad, P. B.; Mokshanatha, P. B.; Hebbar, N.; Venkatesha, V. T.; Tandon, H. C. Ketosulfone Drug as a Green Corrosion Inhibitor for Mild Steel in Acidic Medium. *Ind. Eng. Chem. Res.* **2014**, *53*, 8436−8444.
(47) Cesiulis, H.; Tsyntsaru, N.; Ramanavicius, A.; Ragoisha, G. The Study of Thin Films by Electrochemical Impedance Spectroscopy, Nanostructures and Thin Films for Multifunctional Applications. In *NanoScience and Technology*; Springer International Publishing: Switzerland, 2016; pp 1−41.
(48) Li, X.; Xie, X. Adsorption and inhibition effect of two aminopyrimidine derivatives on steel surface in H_2SO_4 solution. *J. Taiwan Inst. Chem. Eng.* **2014**, *45*, 3033−3045.
(49) Delahay, P.; Susbielles, G. G. Double-layer impedance of electrodes with charge-transfer reaction. *J. Phys. Chem.* **1966**, *70*, 3150−3157.
(50) Macdonald, J. R., Ed. *Impedance Spectroscopy*; John Wiley, 1987; Section 2.2.3.4.
(51) Singh, A. K.; Thakur, S.; Pani, B.; Singh, G. Green Synthesis and Corrosion Inhibition Study of 2-amino-N′-(thiophen-2-yl) methylene) benzohydrazide. *New J. Chem.* **2018**, *42*, 2113−2124.
(52) Xu, B.; Yang, W. Z.; Liu, Y.; Yin, X. S.; Gong, W. N.; Chen, Y. Z. Experimental and theoretical evaluation of two pyridine carboxaldehyde thiosemicarbazone compounds as corrosion inhibitors for mild steel in hydrochloric acid solution. *Corros. Sci.* **2014**, *78*, 260−268.
(53) Bahrami, M. J.; Hosseini, S. M. A.; Pilvar, P. Experimental and theoretical investigation of organic compounds as inhibitors for mild steel corrosion in sulfuric acid medium. *Corros. Sci.* **2010**, *52*, 2793−2803.
(54) Singh, V. P.; Mishra, M.; Tiwari, K.; Singh, A. K. Synthesis, structural and corrosion inhibition studies on Mn(II), Cu(II) and

DOI: 10.1021/acsomega.8b00003
ACS Omega 2018, 3, 4695−4705

Zn(II) complexes with a Schiff base derived from 2-hydroxypropiophenone. *Polyhedron* **2014**, *77*, 57−65.
(55) Durnie, W.; Marco, R. D.; Jefferson, A.; Kinsella, B. Development of a Structure-Activity Relationship for Oil Field Corrosion Inhibitors. *J. Electrochem. Soc.* **1999**, *146*, 1751−1756.
(56) Noor, E. A.; Al-Moubaraki, A. H. Thermodynamic study of metal corrosion and inhibitor adsorption processes in mild steel/1-methyl-4[4(-X)-styryl pyridiniumiodides/hydrochloric acid systems. *Mater. Chem. Phys.* **2008**, *110*, 145−154.
(57) Saha, S. K.; Dutta, A.; Ghosh, P.; Sukul, D.; Banerjee, P. Adsorption and corrosion inhibition effect of Schiff base molecules on the mild steel surface in 1 M HCl medium: a combined experimental and theoretical approach. *Phys. Chem. Chem. Phys.* **2015**, *17*, 5679−5690.
(58) Oguzie, E. E.; Li, Y.; Wang, S. G.; Wang, F. Understanding corrosion inhibition mechanisms—experimental and theoretical approach. *RSC Adv.* **2011**, *1*, 866−873.
(59) Muñoz, A. I.; Antón, J. G.; Guiñón, J. L.; Herranz, V. P. Inhibition effect of chromate on the passivation and pitting corrosion of a duplex stainless steel in LiBr solutions using electrochemical techniques. *Corros. Sci.* **2007**, *49*, 3200−3225.
(60) Ju, H.; Kai, Z. P.; Li, Y. Aminic nitrogen-bearing polydentate Schiff base compounds as corrosion inhibitors for iron in acidic media: A quantum chemical calculation. *Corros. Sci.* **2008**, *50*, 865−871.
(61) Negm, N. A.; Elkholy, Y. M.; Zahran, M. K.; Tawfik, S. M. Corrosion inhibition efficiency and surface activity of benzothiazol-3-ium cationic Schiff base derivatives in hydrochloric acid. *Corros. Sci.* **2010**, *52*, 3523−3536.
(62) Hackerman, N.; Makrides, A. C. Action of Polar Organic Inhibitors. *Ind. Eng. Chem.* **1954**, *46*, 523−527.
(63) Fouda, A. S.; Badr, G. E.; El-Haddad, M. N. The Inhibition of C-steel Corrosion in H_3PO_4 Solution by Some Furfural Hydrazone Derivatives. *J. Korean Chem. Soc.* **2008**, *52*, 124−132.
(64) Singh, D. K.; Kumar, S.; Udayabhanu, G.; John, R. P. 4(N,N-dimethylamino) benzaldehyde nicotinic hydrazone as corrosion inhibitor for mild steel in 1 M HCl solution: An experimental and theoretical study. *J. Mol. Liq.* **2016**, *216*, 738−746.
(65) Li, S. L.; Wang, Y. G. G.; Chen, S. H.; Yu, R.; Lei, S. B.; Ma, H. Y.; Lin, D. X. Some aspects of quantum chemical calculations for the study of Schiff base corrosion inhibitors on copper in NaCl solutions. *Corros. Sci.* **1999**, *41*, 1769−1782.
(66) Taha, M.; Ismail, N. H.; Jamil, W.; Yousuf, S.; Jaafar, F. M.; Ali, M. I.; Kashif, S. M.; Hussain, E. Synthesis, Evaluation of Antioxidant Activity and Crystal Structure of 2,4-Dimethylbenzoylhydrazones. *Molecules* **2013**, *18*, 10912−10929.
(67) Singh, A. K.; Shukla, S. K.; Ahamad, I.; Quraishi, M. A. Solvent-free microwave-assisted synthesis of 1H-indole-2, 3-dione derivatives. *J. Heterocyclic Chem.* **2009**, *46*, 571−574.
(68) Peme, T.; Olasunkanmi, L. O.; Bahadur, I.; Adekunle, A. S.; Kabanda, M. M.; Ebenso, E. E. Adsorption and Corrosion Inhibition Studies of Some Selected Dyes as Corrosion Inhibitors for Mild Steel in Acidic Medium: Gravimetric, Electrochemical, Quantum Chemical Studies and Synergistic Effect with Iodide Ions. *Molecules* **2015**, *20*, 16004−16029.
(69) ASTM G1-03. *Standard Practice for Preparing, Cleaning, and Evaluating Corrosion Test Specimens*; ASTM International: West Conshohocken, PA, 2003.
(70) Singh, A. K.; Quraishi, M. A. Effect of Cefazolin on the corrosion of mild steel in HCl solution. *Corros. Sci.* **2010**, *52*, 152−160.
(71) Singh, A. K.; Quraishi, M. A. Investigation of the effect of disulfiram on corrosion of mild steel in hydrochloric acid solution. *Corros. Sci.* **2011**, *53*, 1288−1297.

DOI: 10.1021/acsomega.8b00003
ACS Omega 2018, 3, 4695−4705